Turkish Journal of Earth Sciences (Turkish J. Earth Sci.), Vol. 18, 2009, pp. 225–238. *Copyright ©TÜBİTAK*
doi:10.3906/yer-0703-3 First published online 04 December 2008

Two-and-Three-Dimensional Crustal Thickness of the Eastern Pontides (NE Turkey)

NAFİZ MADEN[1], KENAN GELİŞLİ[2], YENER EYÜBOĞLU[3] & OSMAN BEKTAŞ[4]

[1] Department of Geological Engineering, Aksaray University, TR–68000 Aksaray, Turkey
(Email: nmaden@aksaray.edu.tr)

[2] Department of Geophysical Engineering, Karadeniz Technical University, TR–61080 Trabzon, Turkey

[3] Department of Geological Engineering, Gümüşhane University, TR–29000 Gümüşhane, Turkey

[4] Department of Geological Engineering, Karadeniz Technical University, TR–61080 Trabzon, Turkey

received 07 March 2007; revised typescript received 12 June 2007; accepted 22 April 2008

Abstract: The Eastern Pontide orogenic belt is divided into three subzones (northern, southern and axial zones) based on present lithologies and facies associations. NE–SW-, NW–SE- and E–W-trending fault systems, which play an important role in palaeotectonics and neotectonics of the Eastern Pontides, separate these zones. Three different methods were used to estimate the Moho depth from observed gravity value, namely (i) empirical relationship between Moho depth and Bouguer anomaly; (ii) spectral analysis of the radial wave number and; (iii) by the gravity inversion method. Power spectrum, a statistical approach, is a widely used technique to determine the depth of geological sources successfully. The empirical linear relations between the Bouguer anomalies and seismically determined crustal thicknesses have been used to compute depths to the Conrad and Moho discontinuities, which are consistent with the average depths obtained from the power spectrum method. The crustal structure was also determined from the inversion of a Bouguer anomaly profile along longitude 39°. Gravity inversion results are consistent with those obtained from the empirical relations and power spectrum methods. We calculated the maximum crustal thickness of 43.8 km in the studied region by using the gravity inversion method, which also showed that crustal thickness increases from north to south.

Key Words: Eastern Pontides, crustal structure, moho depth, Bouguer gravity, gravity inversion

Doğu Pontidler'in (KD Türkiye) 2 ve 3 Boyutlu Kabuk Kalınlığı

Özet: Doğu Pontid orojenik kuşağı kuzeyden güneye doğru litoloji ve fasiyes değişimlerine göre kuzey, güney ve eksen olmak üzere üç alt zona ayrılmaktadır. Doğu Pontidlerin paleotektoniği ile neotektoniğinde önemli rol oynayan KD–GB-, KB–GD- ve D–B-yönlü kırık sistemleri bu zonları birbirinden ayırmaktadır. Doğu Pontid Orojenik Kuşağı'nın kabuk yapısını gravite verisi ile belirlemek için üç farklı yöntem kullanılmıştır. Bunlar (i) moho derinliği ile gravite anomalisi arasında geliştirilen ampirik bağıntı; (ii) güç spektrumu analizi ve (iii) gravite ters özüm yöntemleridir. Güç spektrumu yöntemi istatistiksel bir yaklaşım olup jeolojik yapıların derinliğinin başarılı bir şekilde tespitinde yaygın olarak kullanılmaktadır. Bouguer anomalisi ile sismik yöntemle tespit edilmiş kabuk kalınlığı arasında geliştirilmiş doğrusal ampirik ilişkiler mevcuttur. Doğu Pontidlerin kabuk yapısı 39° boylamı boyunca alınan gravite profiline ters çözüm yöntemi uygulanarak belirlenmiştir. Ters çözüm sonuçları ampirik bağıntılar ve güç spektrumu yöntemiyle elde edilen değerlerle uyumludur. Ters çözüm yöntemi kullanılarak çalışma sahasında maksimum kabuk kalınlığı 43.8 km olarak hesaplanmıştır. Bu çalışma inceleme alanında kabuk kalınlığının kuzeyden güneye doğru arttığını ortaya koymaktadır.

Anahtar Sözcükler: Doğu Pontid, kabuk yapısı, moho derinliği, Bouguer gravite, gravite ters çözüm

Introduction

The Eastern Pontide orogenic belt, a mountain chain 500 km long and 200 km wide, flanking the southeastern coast of the Black Sea, is divided into three subtectonic units: the northern (magmatic arc), southern and axial (back-arc) zones. The northern zone is characterized by upper Cretaceous and Eocene TH-CA magmatic arc volcanics and granitic rocks (Figure 1). In the southern zone Hercynian basement of the Eastern Pontides (Pulur, Agvanis and Tokat massifs), phlogopite and hornblende-bearing mafic-ultramafic intrusions and upper Cretaceous shoshonitic volcanics are exposed. Further south (back-arc basin), mantle peridotites and mid- Cretaceous olistostromal ophiolitic mélange are widespread. NE–SW-, NW–SE- and E–W-trending fault systems, important in the active tectonics of the Eastern Pontides (Bektaş & Çapkınoğlu 1997; Bektaş *et al.* 1999; Eyüboğlu *et al.* 2006) separate these three zones.

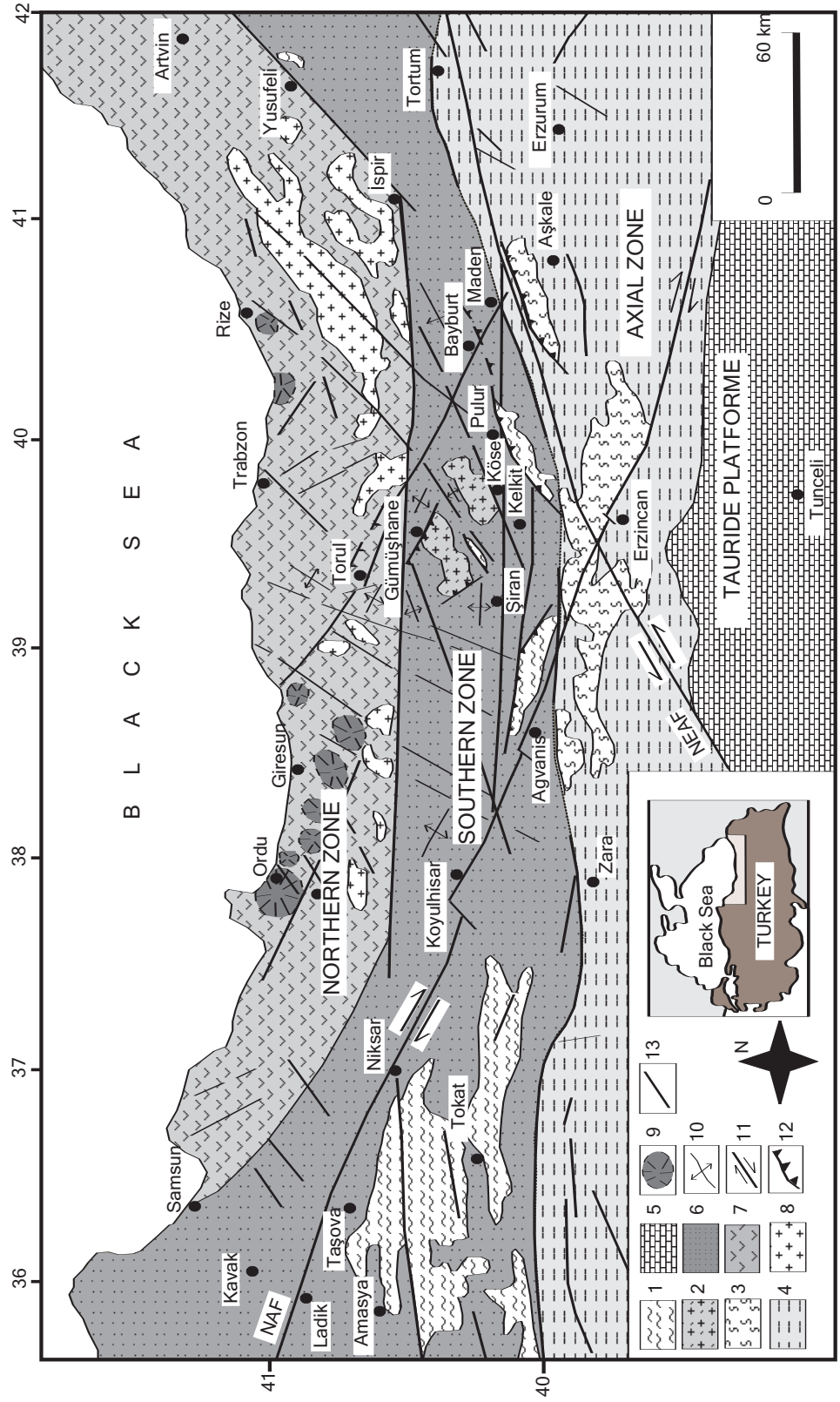

Figure 1. Main tectonic features and tectonic zones of the Eastern Pontides. 1– Palaeozoic metamorphic basement, 2– Palaeozoic granites, 3– serpentinite, 4– undifferentiated Mesozoic and Cenozoic rocks, 5– platform carbonates, 6– mainly Mesozoic sedimentary rocks, 7– Cretaceous and Eocene arc volcanics, 8– upper Cretaceous and Eocene arc granites, 9– caldera or dome, 10– orthogonal drape and drag folds, 11– fault, 12– thrust fault, 13– normal fault, NAF– North Anatolian Fault, NEAF– Northeast Anatolian Fault (Eyüboğlu *et al.* 2006).

Many recent studies have investigated the crustal structure of Anatolia and the surrounding regions (e.g., Mindevalli & Mitchell 1989; Seber *et al.* 2001; Gök *et al.* 2003, 2007; Al-Lazki *et al.* 2003; Zor *et al.* 2003; Pamukcu *et al.* 2007). Zor *et al.* (2003) examined the crustal structure of the Anatolian plateau in Eastern Turkey from the teleseismic recordings of a 29 broadband PASSCAL temporary network, using receiver functions. They calculated an average crustal thickness of 45 km for the entire Eastern Anatolian plateau. Seber *et al.* (2001) stated that most of the Turkish-Iranian plateau is underlain by a crust 45–50 km thick. Therefore, the Turkish-Iranian plateau exhibits a crust thicker than average continental crust, consistent with the evidence for post-late-middle Miocene crustal shortening. Studies of P_n tomographic imaging of mantle velocity and anisotropy by Al-Lazki *et al.* (2003) and regional wave propagation of S_n waves by Gök *et al.* (2003) revealed that the mantle lithosphere is either very thin or completely absent beneath Eastern Turkey. Recently, Gök *et al.* (2007) calculated average crustal thicknesses of 44 km in the Anatolian Block and 48 km in the Anatolian Plateau, while Pamukcu *et al.* (2007) calculated a Moho depth between 38 km to 52 km in Eastern Anatolia.

In this study, we have used three different methods in order to estimate crustal structure of the Eastern Pontides from Bouguer gravity data. These are the power spectrum, empirical relation and gravity inversion methods. Spectral analysis method of potential field data has been widely used to determine the depth of anomaly sources (Bhattacharya 1966; Spector & Grant 1970; Trietel *et al.* 1971; Curtis & Jain 1975; Poudjom Djomani 1992; Chavez *et al.* 1999; Hofstetter *et al.* 2000; Nnange *et al.* 2000; Bansal & Dimri 2001; Lefort & Agarwel 2002; Rivero *et al.* 2002; Gomez-Ortiz *et al.* 2005; Bansal *et al.* 2006). Spector & Grant's (1970) spectral method for estimating mean depth to ensembles of magnetic sources has been generalized to gravity data (Dimitriadis *et al.* 1987) and can be used to map geologic structures from gravity and/or magnetic data observed at the surface (Trietel *et al.* 1971). This technique, which is an easy, fast and affordable method of determining the depths of anomalous sources, gives reliable depth estimates (Nwogbo 1998). When the power spectrum method is applied to the gravity data (Chavez *et al.* 1999; Nnange *et al.* 2000; Lefort & Agarwal 2002), the depths of the crust may be determined and when applied to the magnetic data the Curie point depth may be estimated (Tsokas *et al.* 1998; Ateş *et al.* 2005; Dolmaz *et al.* 2005).

The use of Bouguer gravity data is a common approach to calculate crustal thickness worldwide. Several studies were made and some can be summarized as follows: Pal *et al.* (1979) compiled, based on spectral analysis of Bouguer gravity data, a crustal thickness map of India. Poudjom Djomani *et al.* (1992) applied spectral analyses to Bouguer gravity data to estimate the depth to the major density contrasts within the lithosphere of the Adamawa plateau. The depth between 18 and 38 km corresponds to the crust-mantle interface. Similarly Nnange *et al.* (2000) estimated depths to major lithospherical density contrasts in the entire region of the Adamawa uplift (central Cameroon) by applying 2-D spectral analysis technique on gravity data. The 34 km depth estimate compares well with the 33 km Moho depth. Bansal & Dimri (2001) presented a technique to estimate the depth to anomalous sources from scaling power spectra of long nonstationary gravity profiles. They tested power spectrum technique along a synthetic gravity profile and applied this technique to Jaipur-Raipuer geotransect in western and central India. The geotransect has been divided into four stationary parts. They have interpreted, by using power spectrum technique, four depths of deeper interfaces (37 km, 32 km, 29 km and 31.5 km) that could be the Moho. Lefort & Agarwel (2002) analyzed a complete gravity data set from France and part of the neighbouring countries to compute the topography of the Moho undulations. The last segment being the steepest slope of energy spectrum (33.5 km) corresponds to a mean continental Moho depth. Rivero *et al.* (2002) have tested two different methods to estimate the Moho depth from gravity values. The first one uses an empirical relationship whereas the second one is based on a spectral analysis of the radial wave number using the FFT. In Logarithmic amplitude spectra of the radial wave number graphic, it is possible to observe three straight lines, which give three source depths: 55 km for the deepest, approximately 5 km for the intermediate and 0.32 km for the shallower. Due to density differences, the first one was considered as the Moho discontinuity. Gomez-Ortiz *et al.* (2005) applied a multitaper spectral analysis method to the gravity data of Central Spain to investigate the crustal density structure. Power spectral analysis of this data set reveals the existence of two distinct linear segments. The slope of the

shallowest depth segment (11.6 km) corresponds to the mean depth of the upper crust base and the depth given by the steepest slope (31.1 km) corresponds to the mean Moho depth. Bansal *et al.* (2006) performed a comparative study of depth determination by using three methods of power spectrum computation. The objective of that paper was to study the suitability of the maximum entropy method and multi-taper method in estimating the depth of anomalous sources as compared to the most commonly used FFT method. The thickness of the upper crust found to be at 25–26 km and the Moho depth varies from 39–40 km.

Several studies were made to determine the crust structure from empirical relations (Wollard 1959; Wollard & Strange 1962; Ram Babu 1997; Hofstetter *et al.* 2000; Rivero *et al.* 2002). These empirical relationships between Bouguer anomaly and seismically determined crustal thickness are linearly related, indicating that isostasy prevails on a regional scale (Ram Babu 1997). It is not clear whether the seismic Moho, identified by a change in velocity, and the gravity Moho, marked by a change in density, are at the exactly same depth (Rivero *et al.* 2002). The empirical relations between seismically determined Moho depths and gravity anomaly values are computed in the distinct region and hence, when deciding which relationship to apply on the gravity data of a region it is important to take into account the regional geology and tectonics.

Geological Setting

Anatolia, a seismically active and geologically very complex domain situated in the Alpine-Himalayan orogenic belt, has been defined as a lithospheric continental plate, extruded to the west in response to the N–S relative convergence of Eurasia and Africa-Arabia (McKenzie 1972; Şengör *et al.* 1985; Dewey *et al.* 1986). This lateral tectonic escape (Burke & Şengör 1986) occurs between two strike-slip faults, viz., the dextral North Anatolian (NAF) and the sinistral East Anatolian Fault (EAF), which meet at the Karlıova triangle in Eastern Anatolia (Bozkurt 2001).

The North Anatolian Fault Zone, predominantly a single zone between a few hundred metres to 40 km wide, is one of the best-known strike-slip faults in the world. This transform fault zone runs subparallel to the Black Sea coast and forms part of the boundary between the Eurasian Plate to the north and the Anatolian Plate to the south. This fault zone is also characterized by several second order faults that splay from it into the Anatolian Plate. The EAF, considered to be a conjugate structure to the NAF, is a transform fault forming parts of boundaries between the Anatolian and the Eurasian plates and between the Arabian and African plates (Bozkurt 2001).

The Eastern Pontide orogenic belt is regarded as an example of well-preserved island arcs. There are various opinions about its geotectonic evolution. Dewey *et al.* (1973), Bektaş (1986), Bektaş *et al.* (1999) and Chorowicz *et al.* (1998) supported a southward subduction, whereas Şengör & Yılmaz (1981) proposed a southward subduction model from the Palaeozoic until the Dogger and a northward subduction model from the Late Cretaceous to the end of the Eocene. Yet other authors (Adamia *et al.* 1977; Tokel 1981; Ustaömer & Robertson 1995) proposed that a northward subduction model had generated the Eastern Pontides from the Palaeozoic till the end of the Eocene. Okay & Şahintürk (1997) stated that the opening of the East Black Sea basin is constrained to the Maastrichtian–Paleocene interval and the Eastern Pontides magmatic arc was located close to the present day Black Sea coast during the Maastrichtian.

Bektaş & Güven (1995) suggested that Eastern Pontide magmatic arc consists of serpentinized peridotites, biotite-hornblende-bearing ultramafic-mafic cumulates (lower crust), granitic and metamorphic rocks (middle crust) and bimodal volcanics and intercalated sediments (upper crust) from bottom to top with respect to composition and density of the rocks exposed in the region. Similarly, many studies have been made of the deep structure of other arcs such as Kohistan (Miller & Christensen 1994), Aleutian (Fliedner & Klemperer 1999), Honshu (Kishiro 1987), Talkeetna (DeBari & Sleep 1991).

This study focuses on the determination of the two and three-dimensional crustal structure of the Eastern Pontides using geophysical and geological data.

Data and Methods

The Bouguer anomaly data (Figure 2) of Eastern Pontides, gridded at an interval of 2.5 km, was obtained from the General Directorate of Mineral Research and Exploration (MTA). The study region is bounded between 36°–42° E longitude and 39°–41°.30' N latitude. Gravity

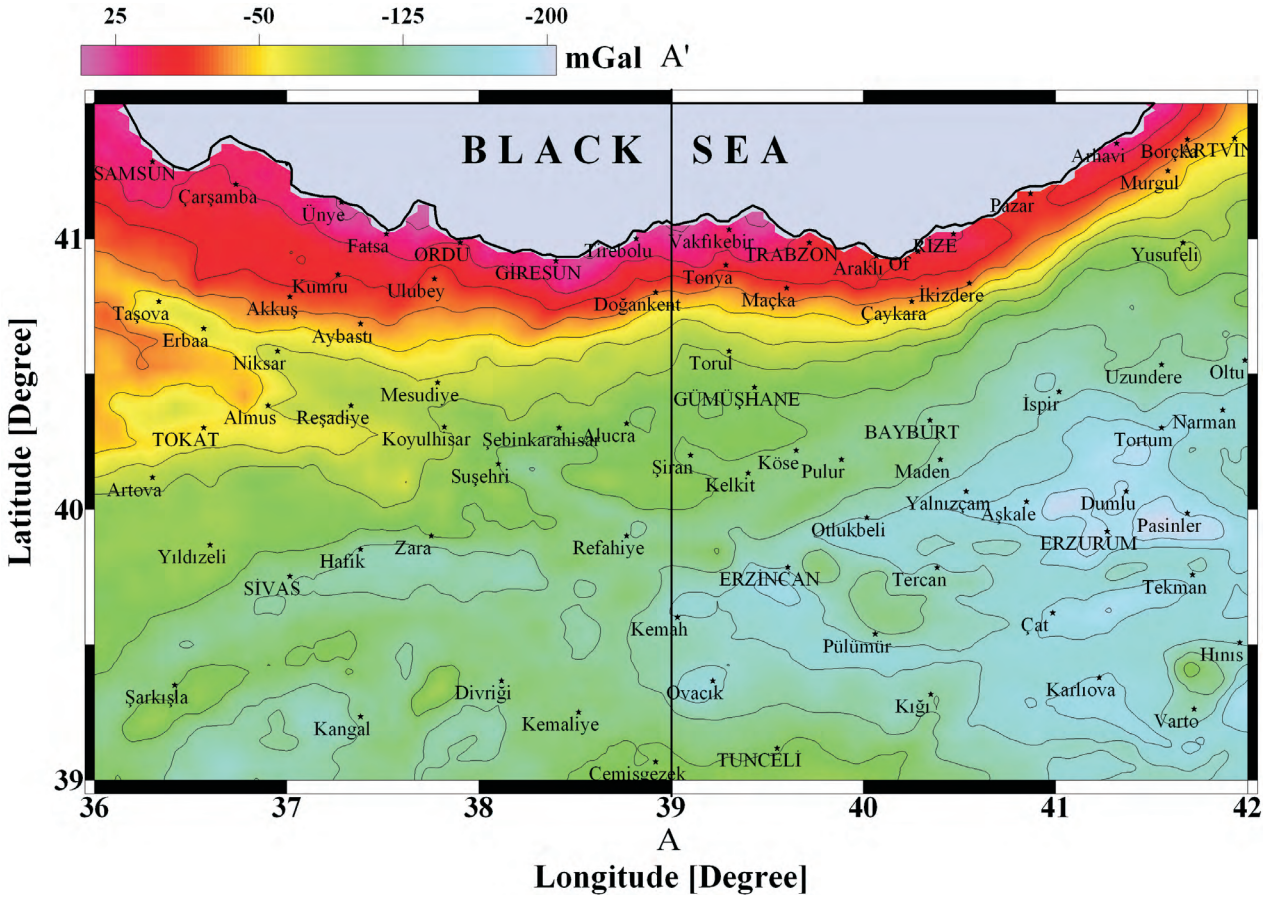

Figure 2. Bouguer gravity anomaly map of the Eastern Pontides. The counter interval is 10 mgal; colour bar at top indicates interval values. Colour levels indicate anomaly intensity from Magenta (positive) to blue (large negative).

values are tied to MTA and General Command of Mapping base stations related to the Potsdam absolute gravity value 981260.00 mGal accepted by the International Union of Geodesy and Geophysics in 1971. Latitude correction was applied according to the Gravity Formulae of 1967. Bouguer reduction was done for a density of 2.40 Mgm^{-3}. Topographic correction was calculated up to a distance of 167 km, assuming a terrain density of 2.67 Mgm^{-3}.

The gravity anomaly, which rose considerably with rising crustal thickness, had evident gravity variation toward the south. Contour lines are parallel to orogenic belt and dominated by a negative anomaly on the anomaly map. Zero contours usually followed the Black Sea coastal line. The southeastern part of the Bouguer anomaly map is almost completely covered by a large negative anomaly due to a sedimentary basin of different age (Maden 2005).

Spector & Grant (1970) established the well-known method to obtain the average depths to the top of magnetized bodies, based on the slope of the log power spectrum. The spectral analysis method provides depth estimation of the top of source bodies from the wavelengths of gravity and magnetic fields (Spector & Grant 1970; Bhattacharyya & Leu 1975, 1977; Pal *et al.* 1979; Poudjom Djomani *et al.* 1992; Chavez *et al.* 1999; Hofstetter *et al.* 2000; Nnange *et al.* 2000; Bansal & Dimri 2001; Lefort & Agarwel 2002; Rivero *et al.* 2002; Gomez-Ortiz *et al.* 2005; Bansal *et al.* 2006). This method does not require a priori knowledge of the geometry and density contrasts of source bodies.

Dimitriadis *et al.* (1987) generalized this approach to gravity data. Trietel *et al.* (1971) used this method to map geological structures from gravity data observed at the surface. In this technique, gravity data is transformed into the wave-number domain to analyze the frequency content of the information. A plot of the logarithm power spectrum versus frequency exhibits several straight-line segments with slope decrease with increasing frequency. The slopes of various segments provide an estimate of the depths to the various levels of anomalous sources. A suitable cut-off frequency separates the power spectrum curve of the Bouguer anomaly into two domains with high and low wavelengths. The high frequency domain is associated with shallow sources and the low frequency domain is related to deeper sources, called residual and regional anomalies, respectively (Spector & Grant 1970).

Following Pal *et al.* (1979), the depth to a given ensemble of prismatic bodies *d*, can be estimated from the power spectrum of the associated anomaly, by applying:

$$E(k,0) = E(0,0)\, e^{\left[\frac{2\pi}{N} d - m\right]k} \qquad (1)$$

where *k, m,* and *N* are the wave number, the slope of the average spectrum and number of gravity data, respectively. The depth, *d*, to the top of the basement can be easily calculated, since the gradient of

$$\left[\frac{2\pi}{N}\, d - m\right]$$

should be zero.

Reagan & Hinze (1976) pointed out that care must be taken to minimize the aliasing errors produced by digitization and to avoid truncating anomalies. The errors in source depth prediction are related closely to the profile length. A profile of six times the expected source depth is required for information loss <10%.

Studies of empirical relationships between Bouguer gravity anomaly (Δg) and seismically determined crustal thickness *(H)* performed by a number of authors (Wollard 1959; Wollard & Strange 1962; Ram Babu 1997; Hofstetter *et al.* 2000; Rivero *et al.* 2002) show a linear relationship. A brief account of the theory on the linear relationship between Δg and H is described below:

Let H_1 and H_2 be the Moho depths at two locations P_1 and P_2 respectively, with corresponding gravity anomalies Δg_1 and Δg_2 (Figure 3). Let σ_c and σ_m be the average densities of the crust and upper mantle, respectively.

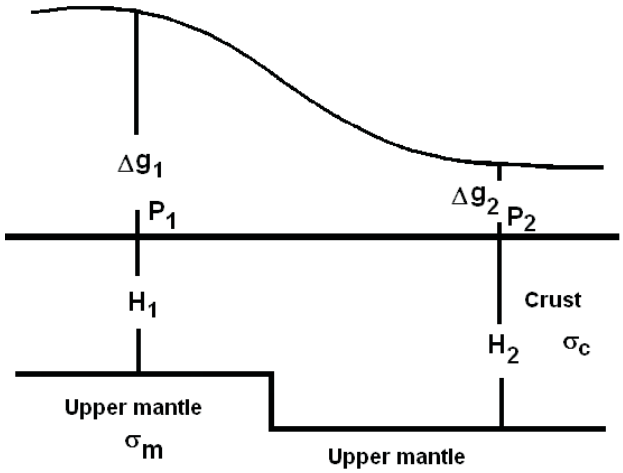

Figure 3. The schematic cross section of a gravity anomaly profile over a density surface (after Ram Babu 1997).

Since $H_2–H_1$, H_1 and $H_2<<x$, where x is the horizontal extent of the structure involved, the maximum gravity anomaly caused by the plate of thickness $H_2–H_1$ is given by

$$\Delta g_1–\Delta g_2 = 2\pi G\,(\sigma_m–\sigma_c)(H_2–H_1), \qquad (2)$$

where G is the Universal gravitation constant. It follows from equation (2) that

$$H_1 = H_2+M(\Delta g_2–\Delta g_1), \qquad (3)$$

where $M = 1/2\pi G(\sigma_m–\sigma_c)$. If H_0 is the Moho depth corresponding to $\Delta g = 0$, equation (3) can be generalized as

$$H = H_0+M\Delta g \qquad (4)$$

This equation represents a straight line with slope M. It is interesting to note that M is directly related to the density contrast ($\sigma_m–\sigma_c$). To calculate the Moho depths from equation (4) a number of DSS profiles must be available in the study region. The M and H_0 constants are determined from a graph of seismic Moho depths against Bouguer values observed in the same stations (Ram Babu 1997).

The gravity inversion method is an exercise trying to fit observed gravity anomalies to the calculated gravity anomalies of a geological model using the least squares method. This technique can be used in other geophysical applications where, very frequently, one deals with non-linear problems. The best fit is defined at the minimum of the objective function, which is the sum of squares of differences between the observed and calculated anomalies.

Any gravity anomaly Δg can be defined by an analytical function $f(x,y,z,a_1,a_2,a_3,...)$ of the space coordinates *x, y, z* of positions of anomalies. In this function $a_1, a_2, a_3, \ldots$ stand for the density parameters for the geological model to calculate the gravity anomaly. The observed gravity anomalies Δg(x,y,z) are available against known *(x, y, z)* coordinate values. The inversion method tries to find out optimum values of $a_1, a_2, a_3, \ldots$such that the gravity anomalies are adequately determined by the function $f(x,y,z,a_1,a_2,a_3,...)$. To fit the calculated gravity anomaly $f(x,y,z,a_1,a_2,a_3,...)$ to the observed gravity anomaly, Δg(x,y,z) a function F is calculated, which is defined by

$$F = \sum_{x,y,z} [g(x,y,z) - f(x,y,z,a_1,a_2,a_3,...] \qquad (5)$$

and the $a_1, a_2, a_3, \ldots$ are identified with minimum *F* (Radhakrishna Murty 1998). We use the strip method in order to calculate the gravity anomalies of the model. In the strip method each vertical cross-section is further replaced by a serious of juxtaposing strips of equal width. The gravity effects of several parallel vertical cross-sections of the geological model are numerically integrated to obtain the gravity anomaly of the geological model.

The gravity inversion method uses the Bouguer gravity values on the AA´ profile to construct the crustal model of the Eastern Pontide orogenic belt. The initial depth of the basalt and granite layers is calculated from empirical equations. Then these values are modified according to the power spectrum values. Finally, the inversion process is fulfilled using iteration. The inversion results at the last iteration that perform the best fit between observed and calculated gravity values have been used for the crust model along the profile.

Determination of the Crustal Structure of the Eastern Pontides

We used power spectrum, empirical relation and inversion methods in estimating the crustal structure of the Eastern Pontides Bouguer anomalies. The power spectrum method is applied to the complete Bouguer gravity anomaly data of the Eastern Pontide orogenic belt.

Logarithmic amplitude spectra of the radial wave number graphic are drawn in order to determine the average depth component of the gravity source. In this graphic, it is possible to observe three straight lines that give three-wave number region and source depths. The low wave number region, between 0 and 0.09 km^{-1}, respecting the contribution of long wavelength sources is considered to be due to density difference at the Moho discontinuity (35.7 km). An intermediate region, in the interval 0.09–0.15 km^{-1}, is associated with the density difference between the upper and lower crust called the Conrad interface (26.5 km). Sediment fill (4.6 km) causes the third region to have wave numbers between 0.15–0.35 km^{-1}. Larger wave numbers (<0.35 km^{-1}) are associated with various errors, having an almost horizontal slope. The depth of 35.7 km may probably correspond to the upper surface of the Moho discontinuity in the north adjacent to the Black sea (Figure 4).

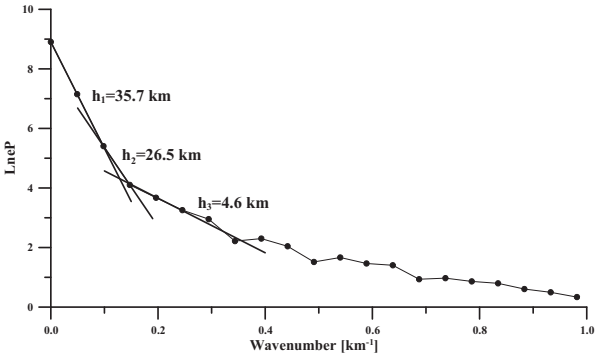

Figure 4. The Power spectrum curves of the Bouguer anomaly of the Eastern Pontides. The values over the linear segments are the depths to various interfaces formed by crustal density contrasts. h_1 represents the Moho depth; h_2 and h_3 represent the depths computed for the main density interfaces within the crust.

A number of studies to determine the crust structure by using empirical relationships between the Bouguer anomaly (Δ*g)* and seismically determined crustal thickness *(H)* reveal that they are linearly related (Wollard 1959; Wollard & Strange 1962; Ram Babu 1997; Hofstetter *et al.* 2000; Rivero *et al.* 2002). In this study, we started with the $H= 32–0.08\ \Delta g$ formula suggested by Wollard (1959) to estimate the Moho depth of the Eastern Pontides. We also used the $H_c= 18.6–0.031\ \Delta g$ (Demenitskaya 1967) equation to calculate the depth of the Conrad surface between the upper and lower crust. The Δ*g* is gravity anomaly, where it should be the difference of two point values. *H* and H_c are the Moho and Conrad depth, respectively. The Conrad values are determined between 25.0 km and 14.6 km (Figure 5) by

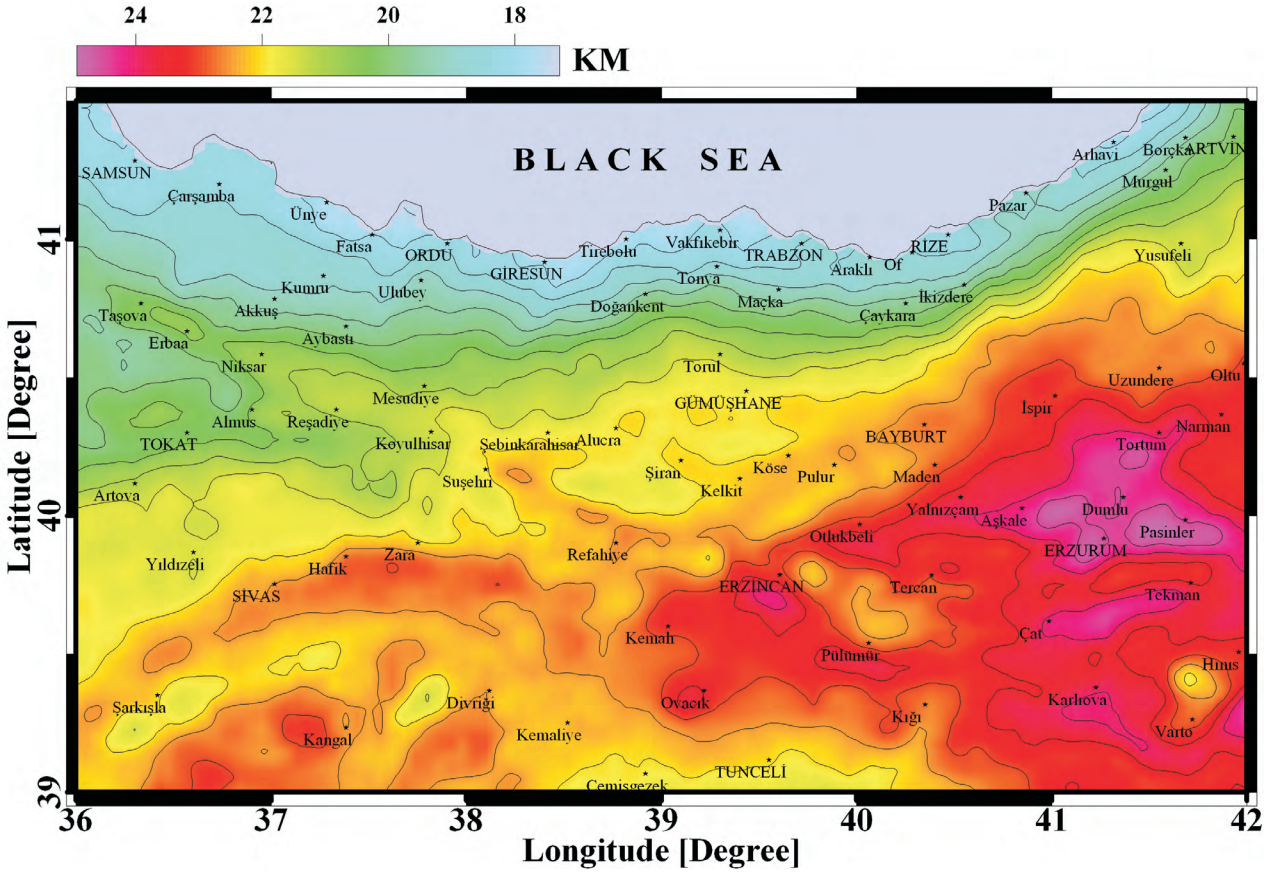

Figure 5. Surface variation maps of Conrad discontinuity of the Eastern Pontides orogenic belt obtained from empirical relationships applying gravity anomaly data of the region. The counter interval is 1 km. Colour levels indicate upper surface depth value of the Conrad and Moho discontinues from magenta (deep) to blue (shallow).

using the $H_c = 18.6–0.031\ \Delta g$ (Demenitskaya 1967) equation. Using the Wollard equation, the average Moho depth is calculated as 28.6 km in the north and 48.4 km in the south (Figure 6). There is 7.1 km difference between Moho depths computed using the power spectrum method and empirical equations. The Wollard equation was suggested for the whole earth instead of a specific region. However, the depth values computed by the Wollard equation give, in general, the information on the crustal thickness in the Eastern Pontides. In addition, it provides an opportunity to compare the results obtained from other methods.

To produce a crustal structure model of the Eastern Pontides, a N–S Bouguer anomaly profile along longitude 39° was selected. The location of the profile (AA´) is shown in Figure 2. Short and long wavelength component anomalies coming from shallow and deep sources were observed on the gravity profile. The long wavelength component was assumed to be caused by crustal thickening. Logarithmic power spectra of the radial wave number of the anomaly profile along the longitude 39° were drawn (Figure 7) to determine the average depth of the anomalous sources in the north and south by considering two distinct depth segments: the first between 0 km to 111 km, the second between 111 km to 222 km.

The energy spectrum analysis (Figure 7) for the gravity data of two distinct segments of profile (AA´) reveals three distinct linear segments. The slopes of the shallowest depth segment (4.1 km in the north segment, 6.2 km in the south segment) may correspond to the mean basin/basement interface. The depths given by the middle segment (19.9 km in the north, 25.0 km in the south) are not far from the depth of the Conrad

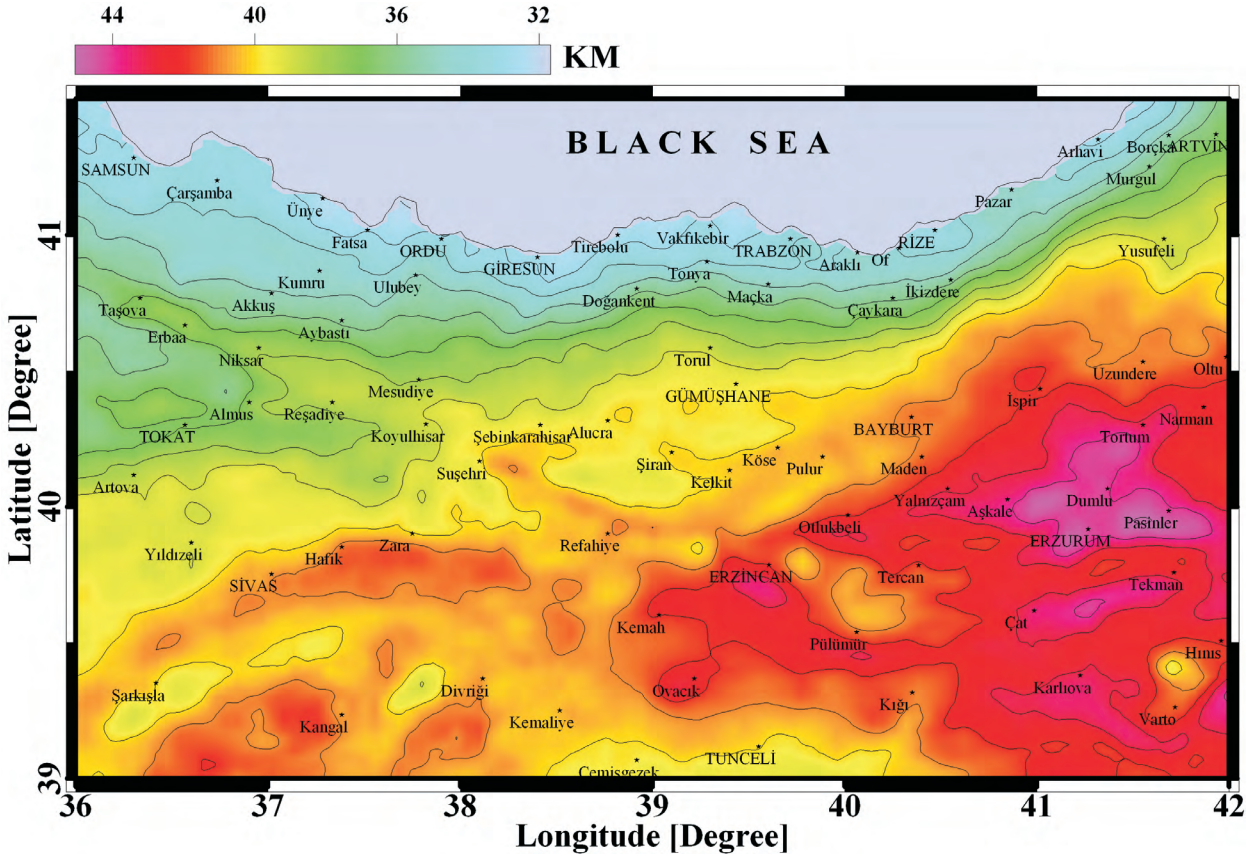

Figure 6. Surface variation maps of Moho discontinuity of the Eastern Pontides orogenic belt obtained from empirical relationships applying gravity anomaly data of the region. The counter interval is 1 km. Colour levels indicate upper surface depth value of the Conrad and Moho discontinues from magenta (deep) to blue (shallow).

discontinuity. The last segment being the steepest slopes (33.9 km in the north, 42.6 km in the south) is attributed to density difference in the Moho discontinuity (Figure 7).

In the inversion study, a three-layered initial crust model comprising granitic, basaltic and crystalline crust was set up. In the model, densities of the mantle, basaltic, granitic and sedimentary layers are assumed, based on the local geology of the region, to be 3.20 Mgm^{-3}, 2.85 Mgm^{-3}, 2.65 Mgm^{-3} and 2.20 Mgm^{-3}, respectively. The initial depths of the basalt and granite layers are calculated from empirical equations. Then these values are modified according to the power spectrum values shown in Figure 4. The best-fit result between the observed and the calculated Bouguer anomaly values are shown in Figure 8 as the crustal model of the region. At the last iteration, while the maximum depth value of the Moho was found to be 43.8 km, the minimum value of the Moho depth was determined as 30.1 km. The minimum and maximum depths of the Conrad discontinuity were found to be 17.4 km and 25.0 km, respectively.

Conclusion

The Eastern Pontide orogenic belt is subdivided into three subzones from north to south identified by their lithologic and facies variations that are justified by gravity data. These three zones are separated from each other by vertical faults which trend NW–SE in the west, are NE–SW-trending in the east and trend E–W in the central part of the Eastern Pontides, which displays the block-faulting tectonic style of the Eastern Pontides (Bektaş & Çapkınoğlu 1997; Eyüboğlu *et al.* 2007). Each block has a distinctive geological evolution. These faults, which bound the blocks, are vertical faults reaching the mantle by splitting the whole crust, as shown by the gravity data variations from north to south in the Eastern Pontides.

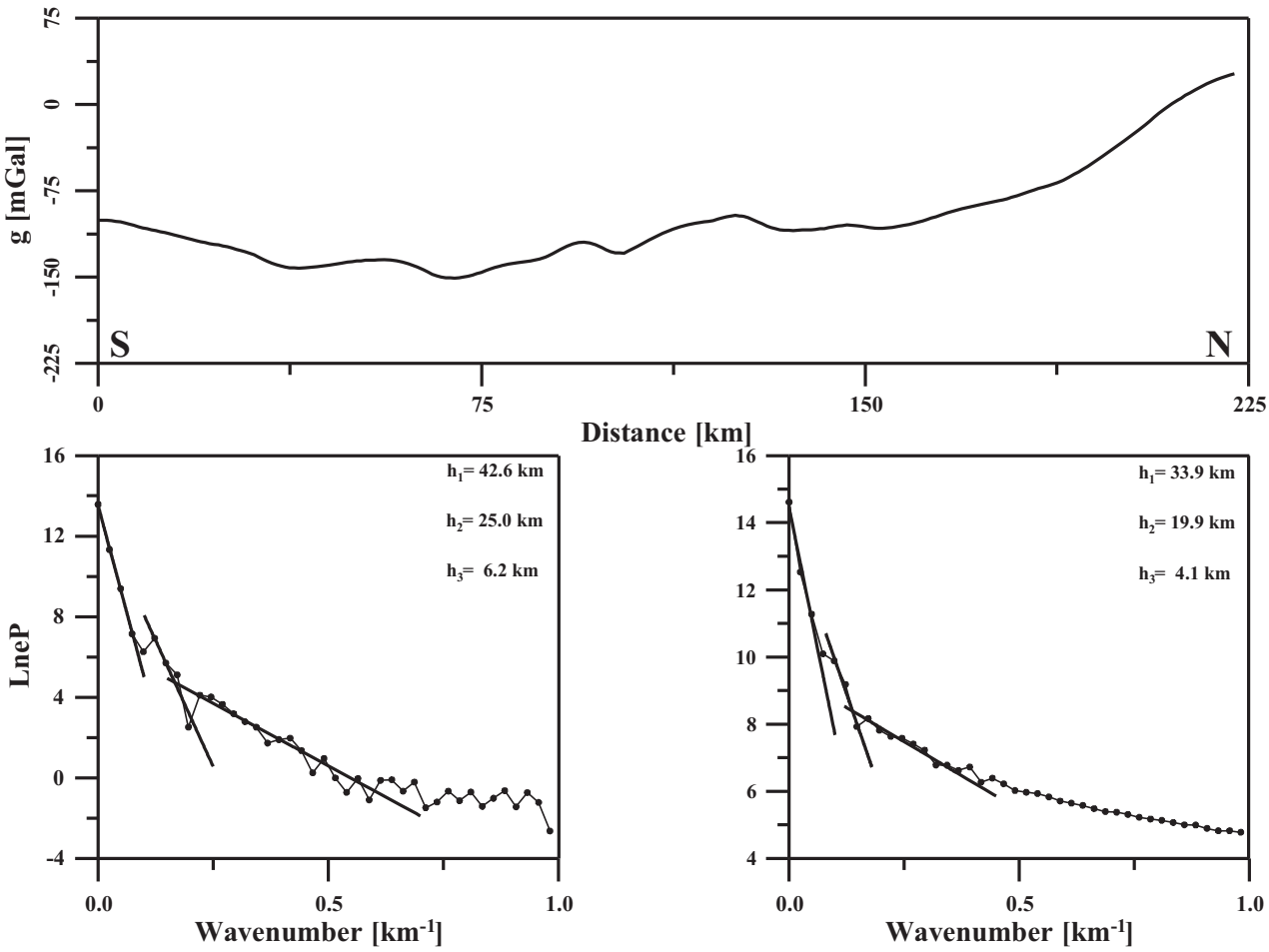

Figure 7. The Power spectrum curves of the Bouguer anomaly profile (AA') along the longitude 39°. The values over the linear segments are the depths to various interfaces formed by crustal density contrasts. h_1 represents the Moho depth; h_2 and h_3 represent the depths computed for the main density interfaces within the crust.

The vertical faults display a flower-structure, with associated shallow low-angle and high-angle faults (Maden 2005; Eyüboğlu *et al.* 2006, 2007). In short, the Eastern Pontide orogenic belt should not be divided into two, but three zones and this view is supported by geological and geophysical data.

In this study, we used three different methods to determine the crustal structure of the Eastern Pontides orogenic belt. The ranges of wavebands in the linear segments of the power spectrum curve have been used to estimate crustal depths. From deepest to shallowest, three depths to the density contrasts are related to crustal horizons.

The energy spectrum analysis (Spector & Grant 1970) for the complete gravity data set (Figure 4) revealed three distinct linear segments. The slope of the shallowest depth segment (4.6 km) may correspond to the mean basin/basement interface. The depth given by the middle segment (26.5 km) may correspond to the density difference between the upper and lower crust. The last segment being the steepest slope (35.7 km) could be the average Moho depth when compared with the inversion results.

In the Eastern Pontide orogenic belt, the depths to the Moho, the Conrad discontinuity and the crystalline basement obtained from power spectrum curve vary from 33.9 km to 42.6 km, 19.9 km to 25.0 km and 4.1 km

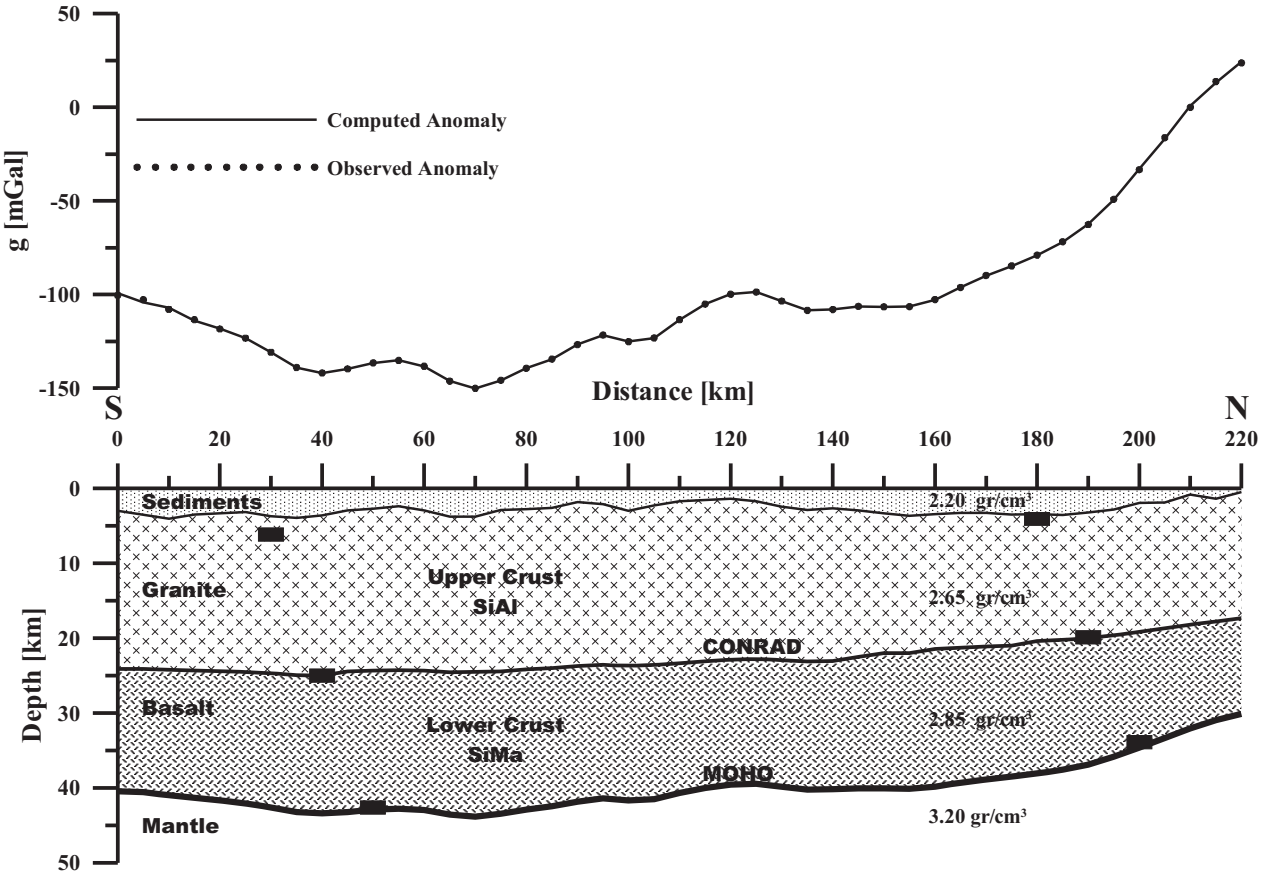

Figure 8. Two-dimensional crustal structure along longitude 39° using gravity inversion methods. The location of the gravity profile is shown in Figure 2. The dotted line shows the initial model; the continuous line shows the final crustal structure obtained from the gravity inversion result. Black boxes on the figure show the power spectrum depth values.

to 6.2 km respectively. Using empirical equations, while the Moho depth was calculated as 28.6 km in the north and 48.4 km in the south, the depth of the Conrad discontinuity was calculated as 25.0 km in the south and 14.6 km in the north. The gravity inversion result showed that depth to the Moho varies from 43.8 km to 30.1 km, and the depth of the Conrad discontinuity between 17.4 km and 25.0 km.

The crustal thickening of the southern and axial zones of the eastern Pontide orogenic belt might be related to the closing of the Neotethys, situated between the Eastern Pontides and the Tauride continent during the Mesozoic, and to the collision of these two continents in the Cenozoic (Şengör *et al.* 2003). However, relative crustal thinning of the northern zone of the Eastern Pontides and its Black Sea continuation must be related to the transition from continental crust to oceanic crust, although the time and formation mechanism of the Black Sea basin is still debated (Bektaş *et al.* 1999).

Because, all methods give a similar depth for the Conrad discontinuity at about 25 km, it is evident that all three different approaches used in this paper produce similar results. If we omit the results determined by empirical equations, there is a 1.8 km difference in the north and a 2.5 km difference in the south between the Moho depth values computed by power spectrum and gravity inversion methods. These values are not far from the results found by Mindevalli & Mitchell (1989); Seber *et al.* (2001); Zor *et al.* (2003); Al-Lazki *et al.* (2003); Pamukcu *et al.* (2007). The maximum difference of the Moho depth values obtained between this study and other studies is 5 km.

Acknowledgements

The Scientific and Technological Researc Council of Turkey (TÜBİTAK) and Karadeniz Technical University Research Grant Fund (20.112.007.1) supported this study. We thank Richard Hansen and anonymous referees for their thorough critical and constructive comments. John A. Winchester edited the English of final text. I express my thanks to General Directorate of the Mineral Research and Exploration (MTA) of Turkey for providing digital gravity data.

References

ADAMIA, S., LORDKIPANIDZE, M.B. & ZAKARIADZE, G.S. 1977. Evolution of an active continental margin as exemplified by the Alpine history of the Caucasus. *Tectonophysics* **40**, 183–189.

AL-LAZKI, A., SANDVOL, E., SEBER, D., TÜRKELLİ, N., MOHAMAD, R. & BARAZANGI, M. 2003. Tomographic Pn velocity and anisotropy structure beneath the Anatolian plateau (Eastern Turkey) and the surrounding regions. *Geophysical Research Letters* **30**, 8043.

ATEŞ, A., BİLİM, F. & BÜYÜKSARAÇ, A. 2005. Curie point depth investigation of Central Anatolia, Turkey. *Pure and Applied Geophysics* **162**, 357–371.

BANSAL, A.R. & DIMRI, V.P. 2001. Depth estimation from the scaling power spectral density of nonstationary gravity profile. *Pure and Applied Geophysics* **158**, 799–812.

BANSAL, A.R., DIMRI, V.P. & SAGAR, G.V. 2006. Depth estimation from gravity data using the maximum entropy method (MEM) and the multi taper method (MTM). *Pure and Applied Geophysics* **163**, 1417–1434

BEKTAŞ, O. 1986. Paleostress trajectories and polyphase rifting in arc-back arc of Eastern Pontides. *Mineral Research and Exploration Institute (MTA) Bulletin* **103/104**, 1–15.

BEKTAŞ, O. & ÇAPKINOĞLU, Ş. 1997. Neptunian dikes and block tectonics in the Eastern Pontide magmatic arc, NE Turkey, implications for the kinematics of the Mesozoic basins. *Geosound* **30**, 451–461.

BEKTAŞ, O. & GÜVEN, İ.H. 1995. Alaskan appinitic type ultramafic and mafic complexes as the root zone of the Eastern Pontide magmatic arc (NE Turkey). *International, Symposium on the Geology of the Black Sea Region, Proceedings*, 189–196.

BEKTAŞ, O., ŞEN, C., ATICI, Y. & KÖPRÜBAŞI, N. 1999. Migration of the upper Cretaceous subduction-related volcanism towards the back-arc basin of the Eastern Pontide magmatic arc (NE Turkey). *Geological Journal* **34**, 95–106.

BHATTACHARYA, B.K. 1966. Continuous spectrum of the total magnetic anomaly due to a rectangular prismatic body. *Geophysics* **31**, 97–121.

BHATTACHARYYA, B.K. & LEU, L.K. 1975. Spectral analysis of gravity and magnetic anomalies due to two-dimensional structures. *Geophysics* **40**, 993–1013.

BHATTACHARYYA, B.K. & LEU, L.K. 1977. Spectral analysis of gravity and magnetic anomalies due to rectangular prismatic bodies. *Geophysics* **42**, 41–50.

BOZKURT, E. 2001. Neotectonics of Turkey – a synthesis. *Geodinamica Acta* **14**, 3–30.

BURKE, K. & ŞENGÖR, A.M.C. 1986. Tectonic escape in the evolution of the continental crust. *In*: BARAZANGI, M. (ed), *Reflection Seismology, Continental Crust, Geodynamic Series, 14*. American Geophysical Union Special Publication, 41–51.

CHAVEZ, R.E., LAZARO-MANCILLA, O., CAMPOS-ENRIQUEZ, J.O. & FLORES-MARQUEZ, E.L. 1999. Basement topography of the Mexicali valley from spectral and ideal body analysis of gravity data. *Journal of South American Earth Sciences* **12**, 579–587.

CHOROWICZ, J., DHONT, D. & ADIYAMAN, Ö. 1998. Black Sea-Pontide relationship: interpretation in terms of subduction. *Third International Turkish Geology Symposium, Abstracts*, p. 258.

CURTIS, C.E. & JAIN, S. 1975. Determination of volcanic thickness and underlying structures from aeromagnetic maps of the Silet area of Algeria. *Geophysics* **40**, 79–90.

DEBARI, S.M. & SLEEP, N.H. 1991. High-Mg, low-Al bulk composition of the Talkeetna island arc, Alaska; implications for primary magmas and the nature of arc crust. *Geological Society of America Bulletin* **103**, 33–47.

DEMENITSKAYA, R.M. 1967. *Crust and Mantle of the Earth*. Nedra, Moscow.

DEWEY, J.F., PITMAN, W.C., RYAN, W.B.F. & BONIN, J. 1973. Plate tectonics and the evolution of the Alpine system. *Geological Society of America Bulletin* **84**, 3137–3180.

DEWEY, J.F., HEMPTON, M.R., KIDD, W.S.F., ŞAROĞLU, F. & ŞENGÖR, A.M.C. 1986. Shortening of continental lithosphere; the neotectonics of Eastern Anatolia, a young collision zone. *In*: COWARD, M.P. & RIES, A.C. (eds), *Collision Tectonics*. Geological Society, London, Special Publications **19**, 3–36.

DIMITRIADIS, K., TSELENTIS, G.A. & THANASSOULAS, K. 1987. A basic program for 2-D spectral analysis of gravity data and source depth determination. *Computers and Geosciences* **13**, 549–560.

DOLMAZ, M.N., HISARLI, Z.M., USTAÖMER, T. & ORBAY, N. 2005. Curie point depths based on spectrum analysis of aeromagnetic data, West Anatolian extensional province, Turkey. *Pure and Applied Geophysics* **162**, 571–590.

EYÜBOĞLU, Y., BEKTAŞ, O., ŞEREN, A., MADEN, N., ÖZER, R. & JACOBY, W.R. 2006. Three-directional extensional deformation and formation of the Liassic rift basins in the Eastern Pontides (NE Turkey). *Geologica Carpathica* **57**, 337–346.

EYÜBOĞLU, Y., BEKTAŞ, O. & PUL, D. 2007. Mid-Cretaceous olistostromal ophiolitic melange developed in the back-arc basin of the eastern Pontide magmatic arc (NE Turkey). *International Geology Review* **49**, 1103–1126.

FLIEDNER, M.M. & KLEMPERER, S.L. 1999. Structure of an island arc: wide-angle seismic studies in the eastern Aleutian Islands, Alaska. *Journal of Geophysical Research* **104**, 10667–10694.

GÖK, R., SANDVOL, E., TÜRKELLİ, N., SEBER, D. & BARAZANGI, M. 2003. Sn attenuation in the Anatolian and Iranian plateaus and surrounding regions. *Geophysical Research Letters* **30**, 8042.

GÖK, R., PASYANOS, M.E. & ZOR, E. 2007. Lithospheric structure of the continent-continent collision zone: eastern Turkey. *Geophysical Journal International* **169**, 1079–1088.

GOMEZ-ORTIZ, D., TEJERO-LOPEZ, R., BABIN-VICH, R. & RIVAS-PONCE, A. 2005. Crustal density structure in the Spanish Central System derived from gravity data analysis (Central Spain). *Tectonophysics* **403**, 131–149

HOFSTETTER, A., DORBATH, C., RYBAKOV, M. & GOLDSHMIDT, V. 2000. Crustal and upper mantle structure across the Dead Sea rift and Israel from teleseismic P-wave tomography and gravity data. *Tectonophysics* **327**, 37–59.

KISHIRO, I. 1987. A petrological model of the mantle wedge and lower crust in the Japanese island arcs. *In*: MYSEN, B.O. (ed), *Magmatic Processes, Physicochemical Principles*. Geochemical Society, London, Special Publications **1**, 165–181.

LEFORT, J.P. & AGARWAL, B.N.P. 2002. Topography of the Moho undulations in France from gravity data: their age and origin. *Tectonophysics* **350**, 193–213.

MADEN, N. 2005. *Doğu Pontid Orojenik Kuşağının Yapı Stillerinin ve Kabuk Yapısının Jeofizik Yöntemlerle İncelenmesi [Geophysical Investigation of Eastern Pontide Orogenic Belt Structural Styles and Crust Structure]*. PhD Thesis, Karadeniz Technical University, Trabzon, Turkey [in Turkish with English abstract, unpublished]

MCKENZIE, D. 1972. Active tectonics of the Mediterranean region. *Geophysical Journal of the Royal Astronomical Society* **30**, 109–185.

MILLER, D.J. & CHRISTIENSEN, N. 1994. Seismic signature and geochemistry of an island arc: a multidisciplinary study of the Kohistan accreted terrene, Northern Pakistan. *Journal of Geophysical Research* **99**, 11623–11642.

MİNDEVALLI, Ö.Y. & MITCHELL, B.J. 1989. Crustal structure and possible anisotropy in Turkey from seismic surface wave dispersion. *Geophysical Journal International* **98**, 93–106.

NNANGE, J.M., NGAKO, V., FAIRHEAD, J.D. & EBINGER, C.J. 2000. Depths to density discontinuities beneath the Adamawa plateau region, Central Africa, from spectral analyses of new and existing gravity data. *Journal of African Earth Sciences* **30**, 887–901.

NWOGBO, P.O. 1998. Spectral prediction of magnetic sources depths from simple numerical models. *Computers and Geosciences* **24**, 847–852.

OKAY, A.İ. & ŞAHİNTÜRK, Ö. 1997. Geology of the Eastern Pontides. *In*: ROBINSON, A.G. (ed), *Regional and Petroleum Geology of the Black Sea and Surrounding Region*. American Associatian of Petroleum Geologists (AAPG) Memoir **68**, 291–311.

PAL, P.C., KHURANA, K.K. & UNNIKRISHNA, P. 1979. Two examples of spectral approach to source depth determination in gravity and magnetics. *Pure and Applied Geophysics* **117**, 772–783.

PAMUKCU, O.A., AKÇIĞ, Z., DEMİRBAŞ, Ş. & ZOR, E. 2007. Investigation of crustal thickness in Eastern Anatolia using gravity, magnetic and topographic data. *Pure and Applied Geophysics*, doi: 10.1007/s00024-007-0267-7.

POUDJOM DJOMANI, Y.H., DIAMENT M. & ALBOUY Y., 1992. Mechanical behaviour of the lithosphere beneath the Adamawa Uplift (Cameroon, West Africa) based on gravity data. *Journal of African Earth Sciences* **15**, 81–90.

RADHAKRISHNA MURTHY, I.V. 1998. *Gravity and Magnetic Interpretation in Exploration Geophysics*. Geological Society of India, Bangalore, India.

RAM BABU, H.V. 1997. Average crustal density of the Indian lithosphere: an inference from gravity anomalies and deep seismic soundings. *Journal of Geodynamics* **23**, 1–4.

REAGAN, R.D. & HINZE, W.J. 1976. The effect of finite data length in the spectral of ideal gravity anomalies. *Geophysics* **41**, 44–55.

RIVERO, L., PINTO, V. & CASAS, A. 2002. Moho depth structure of the eastern part of the Pyrenean belt derived from gravity data. *Journal of Geodynamics* **33**, 315–332.

SEBER, D., SANDVOL, E., BRINDISI, C. & BARAZANGI, M. 2001. Crustal model for the Middle East and North Africa region: implications for the isostatic compensation mechanism. *Geophysical Journal International* **147**, 630–638.

SPECTOR, A. & GRANT, F.S. 1970. Statistical models for interpreting aeromagnetic data. *Geophysics* **35**, 293–302.

ŞENGÖR A.M.C. & YILMAZ Y. 1981. Tethyan evolution of Turkey: a plate tectonic approach. *Tectonophysics* **75**, 181–241.

ŞENGÖR, A.M.C., GÖRÜR, N. & ŞAROĞLU, F. 1985. Strike-slip faulting and related basin formation in zones of tectonic escape: Turkey as a case study. *In*: BIDDLE, K.T. & CHRISTIE-BLICK, N. (eds), *Strike-slip Deformation, Basin Formation and Sedimentation*. Society of Economic Palaeontology and Mineralogy, Special Publications **37**, 227–264.

ŞENGÖR, A.M.C., ÖZEREN, S., ZOR, E. & GENÇ, T. 2003. East Anatolian high plateau as a mantle-supported, N-S shortened domal structure. *Geophysical Research Letters* **30**, 24.

TRIETEL, S., CLEMENT, W.G. & KAUL, R.K. 1971. The spectral determination of depths to buried magnetic basement rocks. *Geophysical Journal of the Royal Astronomical Society* **24**, 415–428.

TOKEL, S. 1981. Plaka tektoniğinde magmatik yerleşimler ve jeokimya: Türkiye'den örnekler [Magma emplacement in plate tectonics and geochemistry: examples from Turkey]. *Yeryuvarı ve İnsan* **6**, 53–65 [in Turkish].

TSOKAS, G.N., HANSEN, R.O. & FYTIKAS, M. 1998. Curie point depth of the island of Crete (Greece). *Pure and Applied Geophysics* **152**, 747–757.

USTAÖMER, T. & ROBERTSON, A.H.F. 1995. Palaeotethyan tectonic evolution of the north Tethyan margin in the Central Pontides, N Turkey. *In*: ERLER, A. & ERCAN, T. (eds), *Proceedings of the International Symposium on the Geology of the Black Sea Region*, 23–42.

WOLLARD, G.P. 1959. Crustal structure from gravity and seismic soundings. *Journal of Geophysical Research* **64**, 1524–1544.

WOLLARD, G.P. & STRANGE, W.E. 1962. Gravity anomalies and crust of the earth in the Pacific basin. *In*: *The Crust of the Pacific Basin*. Geophysical Monograph **6**, 12.

ZOR, E., SANDVOL, E., GÜRBÜZ, C., TÜRKELLİ, N., SEBER, D. & BARAZANGI, M. 2003. The crustal structure of the East Anatolian plateau (Turkey) from receiver functions. *Geophysical Research Letters* **30**, 8044.